THE JOURNAL OF PHYSICAL CHEMISTRY B

Article

pubs.acs.org/JPCB

Thermal Stability, Complexing Behavior, and Ionic Transport of Polymeric Gel Membranes Based on Polymer PVdF-HFP and Ionic Liquid, [BMIM][BF_4]

Shalu, S. K. Chaurasia, R. K. Singh,* and S. Chandra

Department of Physics, Banaras Hindu University, Varanasi-221005, India

ABSTRACT: PVdF-HFP + IL(1-butyl-3-methylimidazolium tetrafluoroborate; [BMIM][BF_4]) polymeric gel membranes containing different amounts of ionic liquid have been synthesized and characterized by X-ray diffraction, scanning electron microscopy, Fourier transform infrared (FTIR), differential scanning calorimetry, thermogravimetric analysis (TGA), and complex impedance spectroscopic techniques. Incorporation of IL in PVdF-HFP polymer changes different physicochemical properties such as melting temperature (T_m), thermal stability, structural morphology, amorphicity, and ionic transport. It is shown by FTIR, TGA (also first derivative of TGA, "DTGA") that IL partly complexes with the polymer PVdF-HFP and partly remains dispersed in the matrix. The ionic conductivity of polymeric gel membranes has been found to increase with increasing concentration of IL and attains a maximum value of 1.6×10^{-2} S·cm^{-1} for polymer gel membrane containing 90 wt % IL at room temperature. Interestingly, the values of conductivity of membranes with 80 and 90 wt % of IL were higher than that of pure IL (100 wt %). The polymer chain breathing model has been suggested to explain it. The variation of ionic conductivity with temperature of these gel polymeric membranes follows Arrhenius type thermally activated behavior.

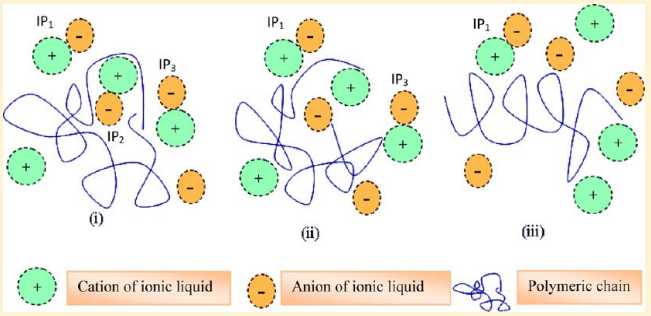

INTRODUCTION

Polymer gel electrolyte membranes have attracted much attention recently due to their high ionic conductivity at room temperature comparable to liquid electrolytes.[1−4] Polymer gel electrolytes can be obtained in two ways: (i) A neutral polymer is added to liquid electrolyte for obtaining highly viscous gel. On further increasing polymer content, free-standing polymer gel membranes can be obtained. (ii) A plasticizing agent such as EC, PC, PEG, ionic liquids, etc. is added to the polymer electrolyte (say polar polymer + salt) which gives plasticized polymer gel electrolyte membrane. These polymeric gel electrolyte membranes possess good mechanical stability as well as high room temperature ionic conductivity of about 10^{-3} S/cm which are useful in solid state electrochemical devices.[5−8] Polymeric gel electrolytes have the advantage of having a higher value of ionic conductivity, being lightweight, and providing good electrode−electrolyte contact as compared to solid polymer electrolyte, which makes them more suitable for solid state electrochemical devices such as batteries, fuel cell, solar cell, double layer capacitor, electrochromic display devices, etc. Polymer gel electrolytes with improved ionic conductivity based on polymer hosts such as PEO, PAN, PMMA, PVdF, and suitable ionic salts with low molecular weight organic solvents EC, PC, DEC, and DMF have been reported.[9−14] These polymeric gel electrolytes are mechanically less stable and not suitable for high temperature operations due to the evaporation of volatile organic solvents.

Recently, the incorporation of ionic liquid into polymer matrices has been used to prepare polymer + ionic liquid gel membranes with high ionic conductivity and mechanical stability.[15−17] The polymer + ionic liquid gel membranes offer several advantages such as the following: (a) high ionic conductivity, (b) wide temperature range of operation, (c) high mechanical stability, (d) wide electrochemical window, etc. Ionic liquids are room temperature molten salts which consist of dissociated cations and anions and have drawn much attention due to some of their remarkable properties such as nonvolatility, high ionic conductivity, good thermal stability, wide electrochemical window, etc.[18] Generally, ionic liquids are liquid at room temperature and, therefore, need to be processed in thin film form suitable for application in solid state electrochemical devices. Many studies[19−21] available in the literature show that ionic liquid can be used as plasticizer to enhance flexibility and hence the ionic conductivity of polymer−salt complexes. However, studies on polymer−ionic liquid gel membranes *without* complexing salt are limited. Some studies are available in which effects of ionic liquid on the properties of polymers, namely, poly(dimethylsiloxane) (PDMS), Nafion and polyurethane−polybutadiene elastomer (PU/PBDO), and poly(vinylidenefluoride-*co*-hexafluoropropylene) (PVdF-HFP), have been studied by combining polymers

Received: August 3, 2012
Revised: November 17, 2012
Published: November 20, 2012

and ionic liquid.[22−25] Polymer gel electrolytes based on the polymer poly(vinylidenefluoride-*co*-hexafluoropropylene) (PVdF-HFP) have been extensively studied because of its high dielectric constant (∼8.4), which facilitates higher dissociation of charge carriers. A few studies[26,27] are available in which ionic liquids [1-(2-hydroxyethyl)-3-MIMBF$_4$] or [1-(2-hydroxyethyl)-3-MIMPF$_6$] or [EMIM][BF$_4$] have been incorporated in polymer PVdF-HFP to obtain free-standing polymer gel membranes.

In this paper, we report the preparation of PVdF-HFP + IL(1-butyl-3-methylimidazolium tetrafluoroborate, [BMIM][BF$_4$]) gel membranes having high ionic conductivity with good mechanical and thermal properties. Different experimental techniques such as XRD, SEM, FTIR, DSC, TGA, impedance spectroscopy, etc. have been used for their characterization. Ionic liquid has been found to partly complex with PVdF-HFP and partly remain entrapped as free IL in the polymeric environment. As a consequence, significant changes in structural, thermal, vibrational, and transport properties are reported and discussed in this paper.

EXPERIMENTAL DETAILS

Materials. Starting materials poly(vinylidenefluoride-co-hexafluoropropylene) [PVdF-HFP], mol wt = 400 000 g/mol, and ionic liquid (IL), 1-butyl-3-methylimidazolium tetrafluoroborate, [BMIM][BF$_4$], were procured from Sigma Aldrich. The ionic liquid was vacuum-dried at ∼10^{-6} torr for 2 days before use.

Synthesis of Polymer−Ionic Liquid Gel Membranes. The PVdF-HFP + IL gel membranes were prepared by conventional solution casting method. For this, a desired amount of polymer PVdF-HFP was dissolved in acetone under stirring at 50 °C until a clear homogeneous solution was obtained. Different amounts of IL (0−90 wt %) were then added in the above solution and again stirred for 2−4 h at 50 °C until a viscous solution of PVdF-HFP + IL was obtained. This was poured into polypropylene Petri dishes for casting. After complete evaporation of the solvent, free-standing rubbery films of polymeric gel membranes containing different amounts of ionic liquid were obtained. All the films were optically transparent.

Surface morphology of the polymeric gel membranes was studied by using scanning electron microscope model Quanta C-200 FEI. The X-ray diffraction profiles of the polymer gel membranes were recorded by Philips X-ray diffractometer model PW 1710 with CuKα1 radiation (λ = 1.540 60 A°) in the range 2θ = 5°−80 °. FTIR spectra of the polymeric gel membranes were recorded with the help of a Perkin-Elmer FTIR spectrometer (model RX 1) between 3500 and 400 cm^{-1}. The differential scanning calorimetery was carried out using a Mettler DSC 1 system in the temperature range 0−200 °C at a heating rate of 10 °C min^{-1}.

Ionic conductivity of the polymeric gel membranes was measured by complex impedance spectroscopy technique using Wayne Kerr precision impedance analyzer, model 6500 B Series, in the frequency range 100 Hz-5 MHz. The bulk resistance was evaluated from complex impedance plots. The electrical conductivity (σ) can be calculated from the following relation

$$\sigma = \frac{1}{R_b} \cdot \frac{l}{A} \qquad (1)$$

where l is the thickness of the sample, A is the cross-sectional area of the sample, and R_b is the bulk resistance obtained from complex impedance plots. For temperature dependent conductivity studies, disc-shaped polymeric gel membranes were placed between two stainless electrodes, and the whole assembly was kept in a temperature controlled oven. The temperature was measured by using a CT-806 temperature controller containing J-type thermocouple. The conductivity of pure ionic liquid was measured by a conductivity cell consisting of two stainless steel plates (area ∼ 1.0 cm^2), separated by 1 cm. The viscosity of the ionic liquid was measured by a Brookfield DV-III Ultra Rheometer in the temperature range −10 to 80 °C. The instrument was calibrated with standard viscosity fluid supplied by the manufacturer before each measurement.

RESULTS AND DISCUSSION

i. Structural Characterization. The addition of ionic liquid or any other plasticizing agent such as PC, EC, etc. is likely to modify the degree of crystallinity and hence the polymer backbone mobility which is partly responsible for enhancing the ionic conductivity. It has been found that ionic liquid, apart from providing mobile ions, also leads to enhanced amorphicity or decreased crystallinity. The structural modification in the polymer involves complexation of the cations of ionic liquid with the polymer backbone which, in turn, affects the degree of crystallinity.

XRD Studies. The X-ray diffraction profiles of pure PVdF-HFP and PVdF-HFP + IL gel membranes containing different amounts of IL are shown in Figure 1. The XRD profile of pure

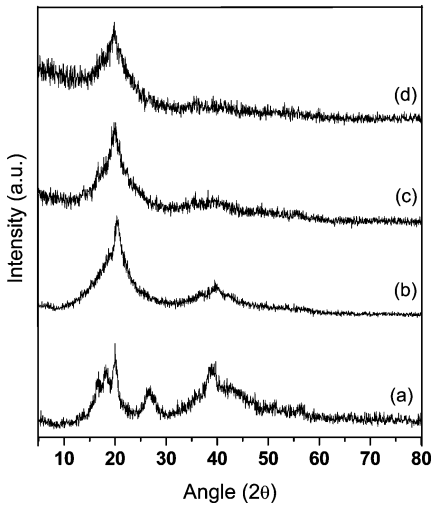

Figure 1. X-ray diffraction profiles of (a) pure PVdF-HFP and PVdF-HFP + x wt % IL gel membranes for (b) x = 30 (c) x = 60, and (c) x = 80, respectively.

PVdF-HFP consists of diffraction peaks at 2θ = 17.94°, 20.05°, 26.42°,and 38.75° (riding over a broad halo), which are respectively assigned to the (100), (020), (110), and (021) reflections of the crystalline plane of α-PVdF.[28] The presence of three peaks indicates partial crystallization of the PVdF units in the copolymer PVdF-HFP giving an overall semicrystalline structure to the copolymer PVdF-HFP.[29] Upon incorporation of IL in the polymer PVdF-HFP, some crystalline peaks of PVdF-HFP disappear, and only two broad peaks/halos at 2θ = 20.47° and 39.93° remain. The XRD profiles of PVdF-HFP + IL gel membranes consist of less intense and broader halos in

dx.doi.org/10.1021/jp307694q | J. Phys. Chem. B 2013, 117, 897−906

comparison to the pure PVdF-HFP. The FWHM of the halo is found to increase with increasing amounts of ionic liquid in the polymer PVdF-HFP. The reduction in intensity and broadening of the peaks for the case of PVdF-HFP + IL gel membranes indicate that the crystallinity of the polymer PVdF-HFP is gradually decreasing upon inclusion of increasing amounts of IL.

SEM Studies. Surface morphology of the prepared PVdF-HFP + IL gel membranes are shown in Figure 2a–c) Pure PVdF-HFP as well as PVdF-HFP + IL gel membranes have solvent swollen structure. The pure PVdF-HFP membrane (see Figure 2a) consists of large crystalline grains with lamellar structure which are uniformly distributed in the membrane. The size of these grains decreases as ionic liquid is incorporated in the polymeric membrane (see Figure 2b). As the amount of IL is increased, the resultant membrane becomes more and more amorphous (see Figure 2c). The evidence of enhanced amorphicity with increasing IL content was also obtained from XRD results as discussed above . The increasing amorphicity also affects the thermal and ion transport behavior which will be discussed later in another section.

ii. Studies of Polymer–Ionic Liquid Complexation by FTIR. In PVdF-HFP + IL gel membranes, possible interaction between the cation of the ionic liquid ($BMIM^+$) and the polymer backbone is likely to change the conformational modes of the polymer backbone. We have used FTIR spectroscopy to investigate the possible ion–polymer interaction and identify the conformational changes in the host polymer PVdF-HFP matrix due to the incorporation of ionic liquid. The FTIR spectra of pure PVdF-HFP, pure IL, and PVdF-HFP + x wt % IL containing different amounts of ionic liquid in the region 3500–400 cm^{-1} are given in Figure 3A. Three regions, viz., region I, region II, and region III, in the spectra of Figure 3A are of particular interest for the present discussion. The expanded version of region I along with the peak positions are given in Figure 3B. The peak positions of region II are discussed later in this section. The region III belongs to the C–H stretching vibration of imidazolium cation ring, which is more likely to be affected due to complexation. Hence, a detailed deconvolution has been done for this region and is given later in Figure 4. Conclusions drawn from region I, region II, and region III are discussed below.

The expanded spectra of region I are shown in Figure 3B. The vibrational bands of pure polymer PVdF-HFP (see curve a) observed at 491, 513, 531, 614, 762, 796, and 976 cm^{-1} are due to the crystalline phase (α-phase) of the polymer PVdF-HFP, while the bands at 841 and 879 cm^{-1} are related to amorphous phase (β-phase) of the polymer. The bands appearing at 491 and 513 cm^{-1} are related to the bending and wagging vibrations of the CF_2 group, while the band at 614 cm^{-1} is the mixed mode of CF_2 bending and CCC skeletal vibration. The band at 762 cm^{-1} is related to the CH_2 rocking vibration. The peaks appearing at 976 and 531 cm^{-1} are due to nonpolar trans–gauche–trans–gauche′ (TGTG′) conformation, and the band at 796 cm^{-1} is due to CF_3 stretching vibration of PVdF-HFP. The band at 841 cm^{-1} is assigned to the mixed mode of CH_2 rocking and CF_2 asymmetric stretching, while the band at 879 cm^{-1} is due to combined CF_2 and CC symmetric stretching vibrations.[30−35] Upon incorporation of IL in the polymer PVdF-HFP, all the intense bands of pure PVdF-HFP crystalline phase (i.e., α-phase), viz., 976, 796, 762, 614, and 531 cm^{-1}, start disappearing and/or becoming weak. Interestingly, the peaks at 841 and 879 cm^{-1} belonging to the amorphous phase (β-phase) become prominent. This shows that IL increases the amorphicity of the polymer film, a conclusion which was also drawn from XRD results discussed earlier. The peak at 513 cm^{-1} lies very near to the peak of IL at ~522 cm^{-1} (marked with arrow ↑ in curve b

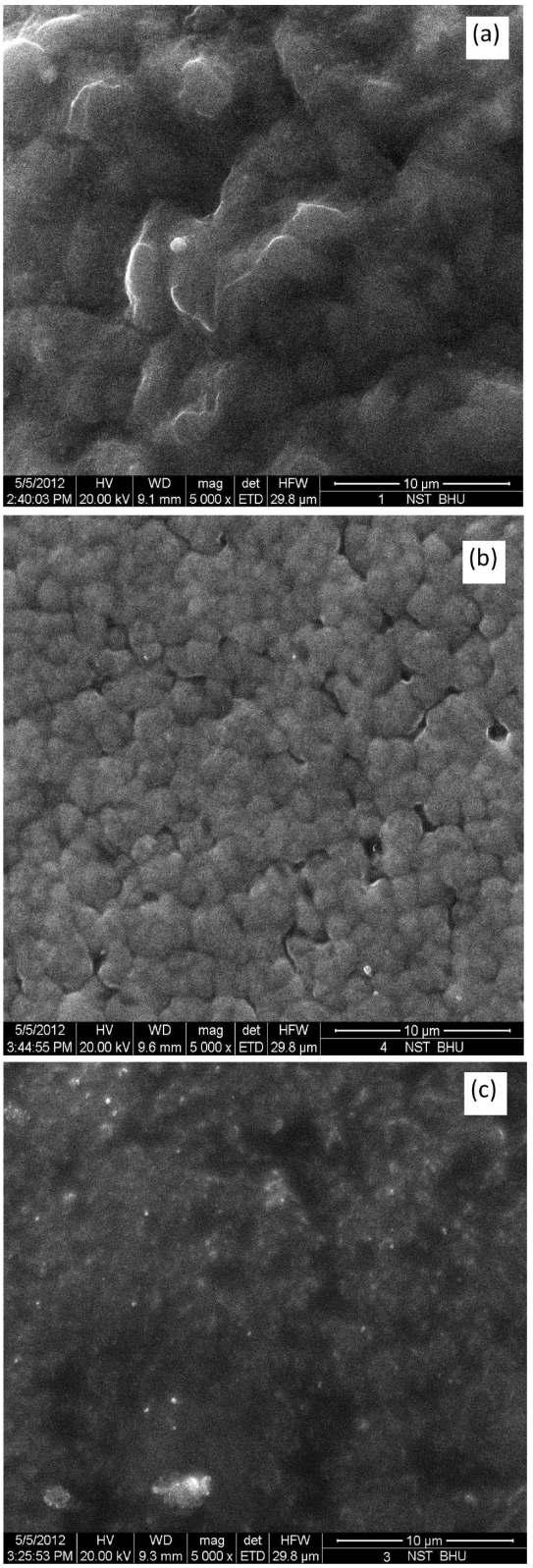

Figure 2. SEM micrograph for (a) PVdF-HFP, (b) PVdF-HFP + 30 wt % IL, and (c) PVdF-HFP + 80 wt % IL gel membranes.

dx.doi.org/10.1021/jp307694q | J. Phys. Chem. B 2013, 117, 897–906

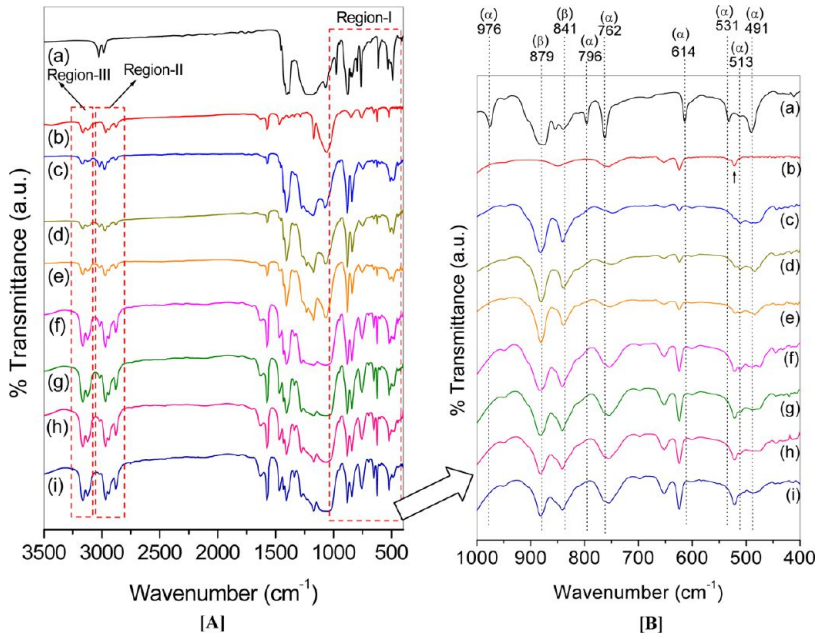

Figure 3. (A) FTIR spectra of (a) pure PVdF-HFP, (b) pure IL, and PVdF-HFP + x wt % IL gel membrane for (c) x = 10, (d) x = 20, (e) x = 30, (f) x = 40, (g) x = 50, (h) x = 60, and (i) x = 70 in the region 3500−400 cm^{-1}. (B) Expanded spectra for the above in the region 1000−400 cm^{-1}. The peaks at 976, 762, 614, 531, and 513 cm^{-1} are due to the crystalline or α-phase of PVdF-HFP; peaks at 879 and 841 cm^{-1} are for amorphous or β-phase of PVdF-HFP.

of Figure 3B). Hence, they tend to merge and no definite conclusion can be drawn from this peak. The peak at 491 cm^{-1} also weakens and splits into two peaks indicating appearance of an additional conformation of the polymer.

The peaks in the region II and region III (as shown by the dotted portion in Figure 3A) in the spectral range 3200−2800 cm^{-1} are respectively due to the C−H stretching vibrations of butyl chain of IL (also those of polymer backbone stretching) and imidazolium cation ring of IL.[36−38] A study of these bands can give information about the complexation due to incorporation of IL in the polymeric matrix. The C−H stretching vibrations of polymer backbone (see curve a in Figure 3A) are at 2985 and 3026 cm^{-1}, while for pure IL, three peaks at 2966, 2939, and 2879 cm^{-1} in the region II are due to the alkyl C−H stretching of butyl chain of IL. The respective peak positions in the PVdF-HFP + IL gel membranes are given in Table 1. It can be seen that C−H stretching vibrations related to the butyl chain of IL at 2879 and 2939 cm^{-1} do not shown significant change. The peak at 2966 cm^{-1} cannot be clearly seen since it is near the peak of polymer chain vibration at 2985 cm^{-1}. This indicates that the butyl chain is not complexing with the polymer backbone (it is the imidazolium cation ring of IL which complexes with the polymer backbone as discussed in the next paragraph). However, complexation of the polymer backbone with IL decreases the polymer C−H vibrations at 3026 and 2985 cm^{-1}. The shift for the latter is larger , and this vibrational frequency monotonically decreases to 2969 cm^{-1} with increasing IL content.

In view of the above discussions, we also expect significant changes in the C−H stretching vibration related to imidazolium cation ring[39−41] which lie in the region III of Figure 3[A]. We have carried out a detailed deconvolution of the spectra of region III in the spectral range 3225 to 3075 cm^{-1} in order to find exact peak positions of C−H stretching vibrations of imidazolium cation ring to ascertain the role of IL complexation. The deconvolution was done with the help of Peakfit software.[42] In all the cases, the deconvolution was carried out using multiple Gaussian peaks to extract the exact peak positions of PVdF-HFP + IL gel membranes. The deconvoluted spectra of pure IL and PVdF-HFP + IL gel membranes containing different amounts of IL are given in Figure 4. The reliability of deconvolution is reflected in the values of the square of regression coefficient r which was ≈0.999 as given in Figure 4a−h. The deconvoluted FTIR spectra of pure IL consists of a strong peak at 3163 cm^{-1} (marked as X_1 in Figure 4a) and two relatively less intense peaks at 3106 and 3125 cm^{-1}. The deconvoluted spectra of PVdF-HFP + IL gel membranes consist of an additional peak at ∼3176 cm^{-1} (marked as X_2 in Figure 4b). In PVdF-HFP + IL gel membranes, IL could be present in two different environments, viz., (i) IL cation complexed with the polymer chain and (ii) excess uncomplexed IL. The peaks X_1 and X_2 in Figure 4b−h are assigned respectively to these. It can be seen that the 3163 cm^{-1} peak of pure IL (indicated as X_1 peak in Figure 4a) shifts to 3161→3159→3159→ 3158→ 3157→3156→3155 as the IL content is increasing from 10 to 70 wt % as shown in Figure 4b−h. Further, we expect that the "amount" of uncomplexed IL (X_2 peak) will be more if the overall content of IL is more in the polymer PVdF-HFP. We can see that the intensity of the peak X_2 increases as the IL content is increasing. We can see from Figure 5 that the X_2/X_1 intensity ratio is increasing with the concentration of IL. At lower content of added IL in polymer gel membrane, most of the IL complexes with the polymer and less uncomplexed IL is entrapped in the matrix. As the concentration of IL in the polymer gel membrane increases, the amount of uncomplexed IL increases leading to monotonic increase in the intensity of peak X_2 with IL content. The above discussions clearly indicate that conformational changes are occurring in the polymer PVdF-HFP after complexation with IL. These may be reflected in the thermal behavior of the polymeric membranes. So, we carried out thermal studies (DSC and TGA) which are discussed below.

dx.doi.org/10.1021/jp307694q | J. Phys. Chem. B 2013, 117, 897−906

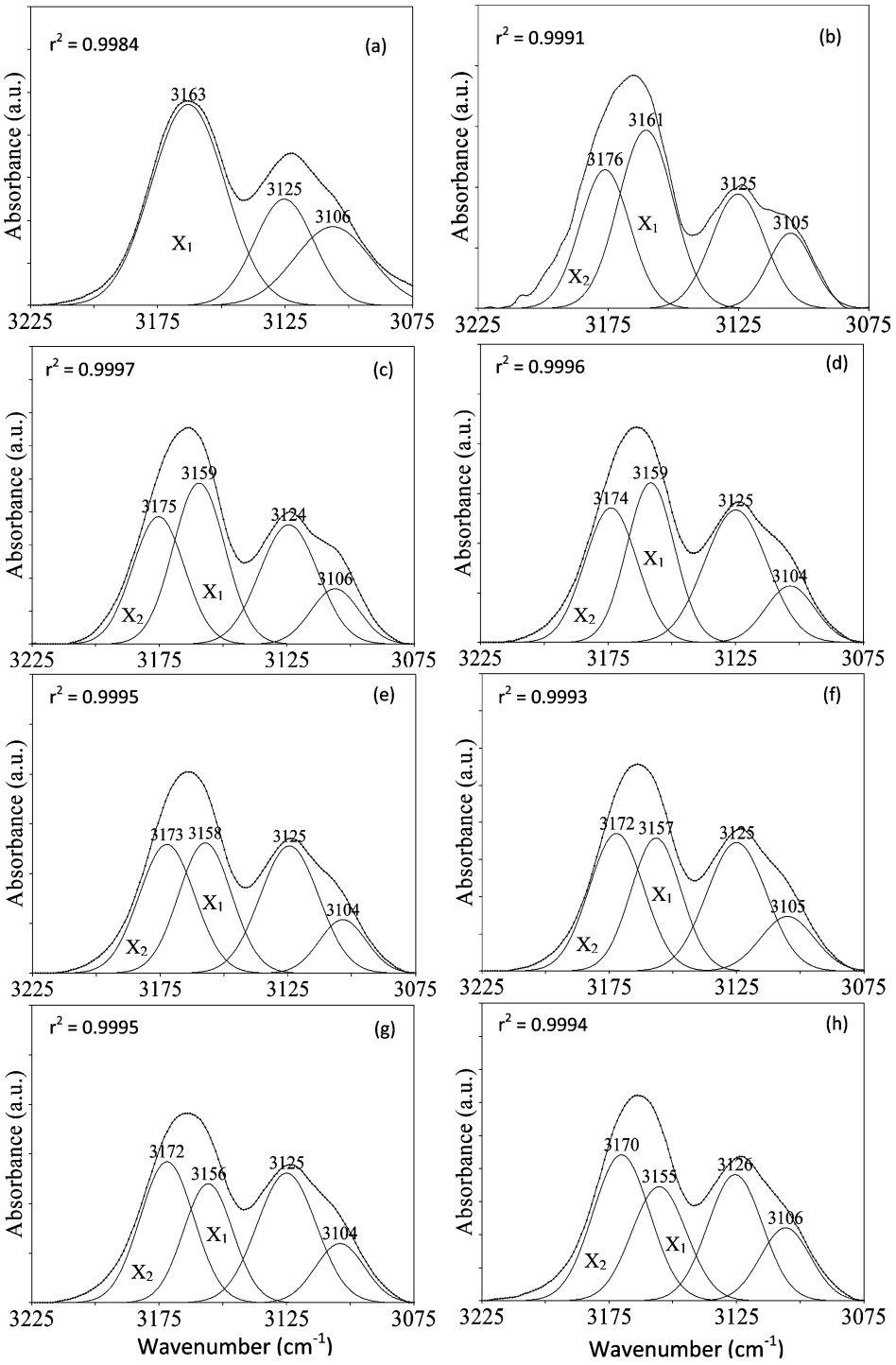

Figure 4. Deconvoluted FTIR spectra of (a) pure IL and PVdF-HFP + x wt % IL gel membranes for (b) x = 10, (c) x = 20, (d) x = 30, (e) x = 40, (f) x = 50, (g) x = 60, and (h) x = 70 for CH stretching vibrational mode of imidazolium cation ring of IL in the region 3225−3075 cm^{-1}.

Table 1. Peak Positions of Vibrational Bands in Region II for Pure PVdF-HFP, Pure IL, and PVdF-HFP + x wt % IL Gel Membranes for x = 0−70 in cm^{-1}

		PVdF-HFP + x wt % IL						
PVdF-HFP	pure IL	10	20	30	40	50	60	70
3026	–	3021	3021	3021	3019	3019	3019	3019
2985	–	2977	2973	2970	2970	2970	2969	2969
–	2879	2881	2881	2881	2881	2880	2880	2880
–	2966	–	–	–	–	–	–	–
–	2939	2942	2941	2941	2941	2940	2940	2940

dx.doi.org/10.1021/jp307694q | J. Phys. Chem. B 2013, 117, 897−906

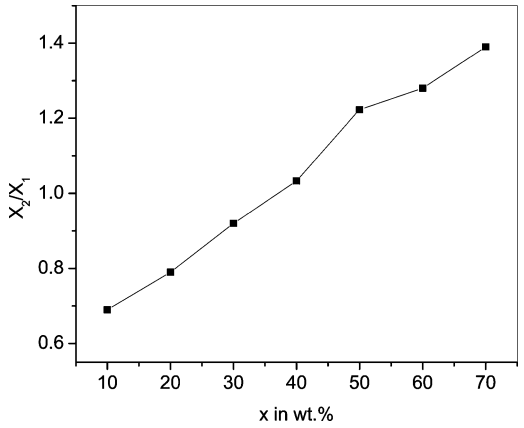

Figure 5. Ratio of the relative intensities of uncomplexed to the complexed IL (X_2/X_1) vs concentration of IL in PVdF-HFP + x wt % IL gel membranes for different values of x.

iii. Effect of Ionic Liquid on Thermal Behavior of Polymer PVdF-HFP: DSC and TGA Studies. The DSC thermograms of pure PVdF-HFP and PVdF-HFP + IL gel membranes containing different amounts of ionic liquid are shown in Figure 6. An endothermic peak corresponding to the

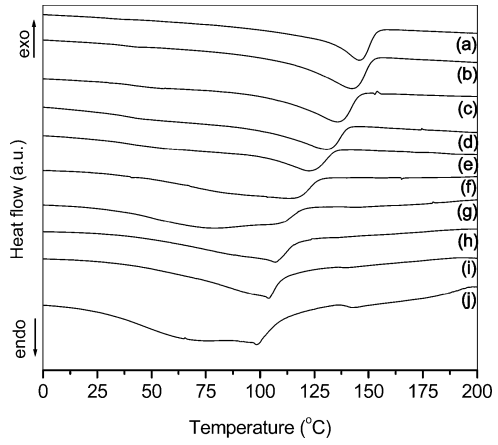

Figure 6. DSC thermograms for (a) PVdF-HFP and PVdF-HFP + x wt % IL gel membranes for (b) x = 10, (c) x = 20, (d) x = 30, (e) x = 40, (f) x = 50, (g) x = 60, (h) x = 70, (i) x = 80, and (j) x = 90, respectively.

melting of crystalline phase[43] of polymer PVdF-HFP is observed at 143 °C (see Figure 6a). The melting temperature (T_m) of the PVdF-HFP shifts to lower values on incorporation of different amounts of IL as shown in Figure 6b–j. The shifts in the values of T_m of the polymer–ionic liquid gel membranes are due to the plasticization effect of IL as well as due to its complexation with the polymer backbone. This observation is in conformity with the XRD and SEM results discussed earlier.

Figure 7 shows the thermogravimetric analysis (TGA) and derivatives of thermogravimetric (DTGA) curves of pure PVdF-HFP, pure IL along with the TGA and DTGA curves for PVdF-HFP + IL gel membranes containing different amounts of ionic liquid. Pure PVdF-HFP decomposes at ~475 °C, and pure IL decomposes at 470 °C (see Figure 7a and b). Both these decompositions are single step. However, the PVdF-HFP + IL gel membranes exhibit a multistep decomposition mechanism as shown in Figure 7. It may be remarked here that at lower content of ionic liquid (up to 20 wt %), the decomposition temperature of polymer and IL cannot be separated out. However, at higher concentrations (30 and 40 wt %) of IL in PVdF-HFP + IL gel membrane, two decomposition peaks (P_1 and P_2) are observed (see Figure 7c–d). On further increasing the content of IL, two things happen: (i) relative intensity of P_1 increases and (ii) P_2 gets splitted into two peaks P_2 and P_2' (see Figure 7e–h). The FTIR results discussed earlier in this paper have shown that IL partly complexes with the polymer chain and partly remains as entrapped IL, and the amount of the latter increases as the IL content in the membrane increases. Guided by this result, we attribute P_1 to the entrapped IL (since the intensity of P_1 is increasing with increasing IL content). The peak P_2 is due to the decomposition of pure PVdF-HFP, while P_2' corresponds to the decomposition of PVdF-HFP complexed with IL, evidence for the presence of which also existed in our FTIR results. Further, it may be noted that, at higher IL content, most of PVdF-HFP backbone gets complexed and hence the P_2' grows at the expense of P_2.

iv. Ionic Transport Studies. The ionic conductivity (σ) of pure IL is 5.9 × 10^{-3} S·cm^{-1} at 30 °C which increases with increasing temperature as shown in Figure 8. This increase in conductivity is closely related to the decrease in viscosity with temperature (as given in Figure 8), which leads to an increase in ionic mobility.

The conductivity of IL is expected to decrease as polymer is added to it. The composition dependent ionic conductivity of PVdF-HFP + IL polymeric gel membranes with different amounts of added polymer PVdF-HFP is shown in Figure 9. Contrary to our expectation, it is found that the ionic conductivity initially increases at lower content of added polymer PVdF-HFP (say 10 wt %) in IL, and then it starts to decrease monotonically at higher concentrations of polymer. The addition of polymer in ionic liquid obviously will increase the viscosity of the ionic liquid which should ordinarily lead to a decrease in the ionic mobility, and hence conductivity. But in our case, we notice an enhancement in conductivity value at lower concentration (~10 wt %) of added polymer PVdF-HFP in ionic liquid. Grillone et al.[44] have also observed an increase in the ionic conductivity value on their proton conducting polymeric gel membranes based on salicylic acid and polymer PMMA after gellification. Patel et al.[45] have also reported that the conductivity of a cross-linked polymer gel electrolyte based on polymerized acrylonitrile with added ionic liquid did not decrease even though the viscosity increased due to the addition of polymer. They argued that "the transformation from disorder (ionic liquid) to a relatively ordered cross-linked polymer electrolyte phase does not at all influence the concentration of conducting species and the polymer framework is still able to provide efficient path ways for fast ion transport". Chandra et al.[46] have earlier suggested a "qualitative" explanation for conductivity behavior of polymer gel electrolytes based on "chain breathing model" where they argue that the ion pairs normally present in liquid electrolyte break in the presence of polymer. The increase in the number of charge carriers due to ion pair breaking compensates for the decrease in ionic mobility due to enhanced viscosity caused by addition of polymer. Figure 10 systematically shows polymeric chains dispersed in IL which primarily consists of dissociated cation and anion along with some ion pairs (IP_1, IP_2, and IP_3 etc.). As the polymer chains breathe and open up, they occupy different volumes. In the process of opening up (see Figure 10 (ii) and (iii), where IP_1 and IP_2 are shown to be broken), this

dx.doi.org/10.1021/jp307694q | J. Phys. Chem. B 2013, 117, 897–906

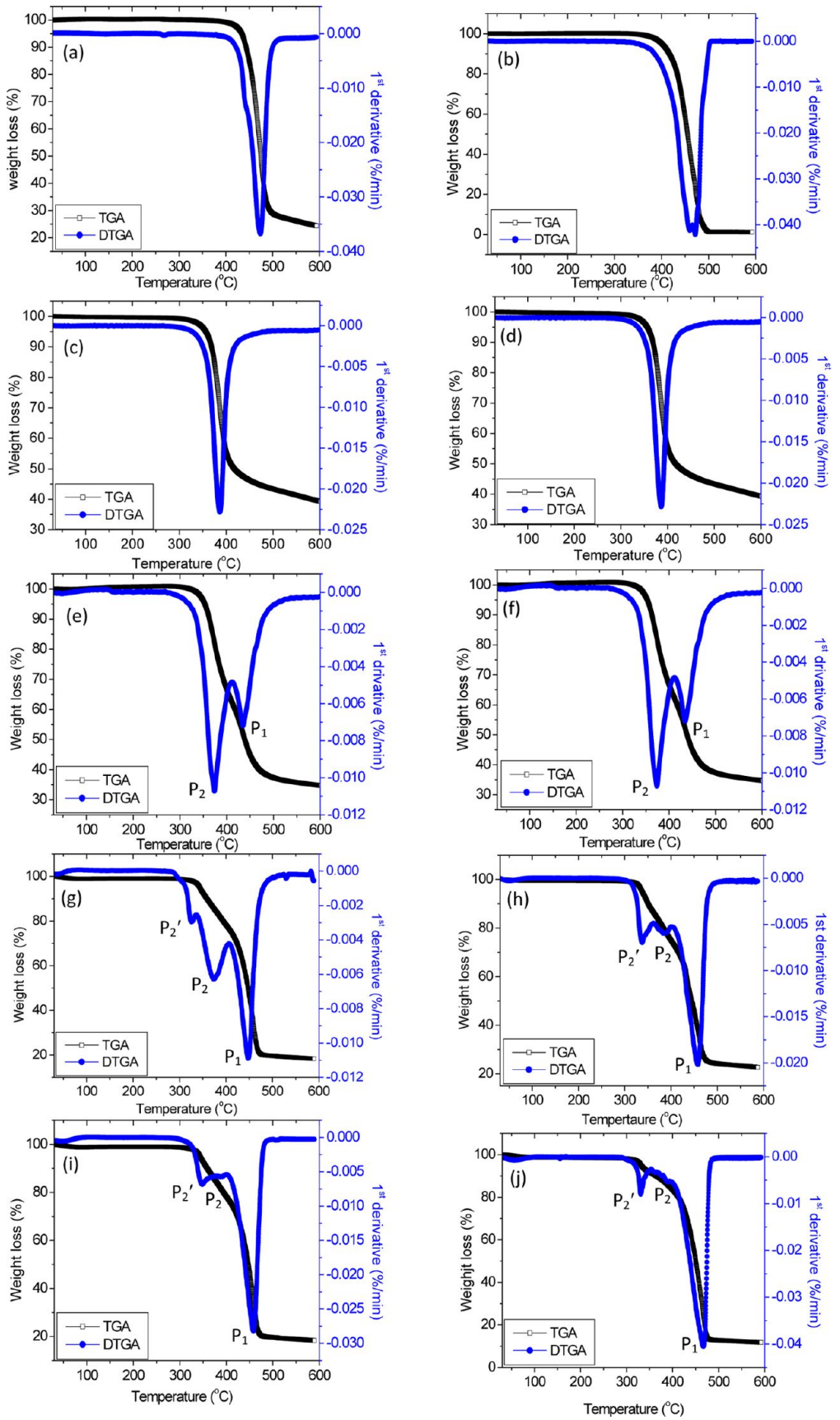

Figure 7. TGA and DTGA curves for (a) pure PVdF-HFP, (b) pure IL, and PVdF-HFP + *x* wt % IL gel membrane for (c) *x* = 10, (d) *x* = 20, (e) *x* = 30, (f) *x* = 40, (g) *x* = 50, (h) *x* = 60, (i) *x* = 70, and (j) *x* = 80, respectively.

dx.doi.org/10.1021/jp307694q | J. Phys. Chem. B 2013, 117, 897−906

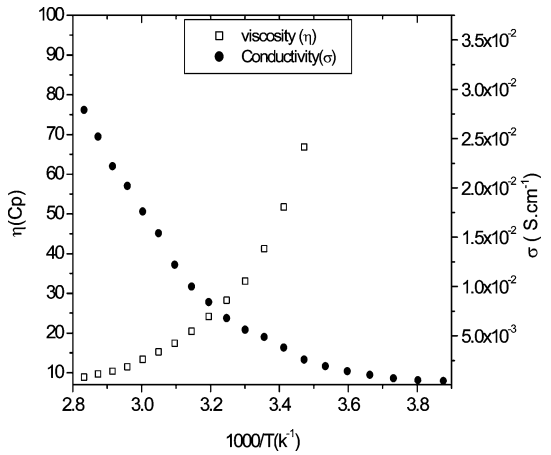

Figure 8. Temperature dependent conductivity and viscosity of pure IL.

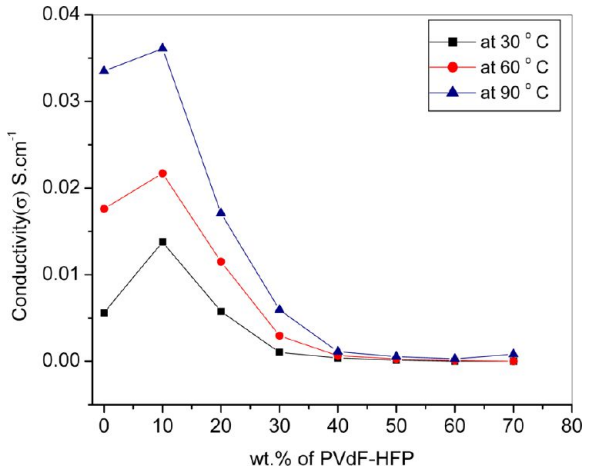

Figure 9. Variation of ionic conductivity of IL with different amounts (0–70 wt %) of polymer PVdF-HFP at three different temperatures.

leads to changes in the local pressure which either breaks the ion pairs or produces unblocking of the viscosity controlled mobility, both resulting in enhancement of the ionic conductivity. The breakup of ion pairs leads to an increase in the number of free charge carriers (and hence conductivity). However, if the content of added polymers is too high, then the viscosity effect would dominate, which decreases the conductivity as observed by us (see Figure 9).

The temperature dependent ionic conductivity of PVdF-HFP + IL gel membranes containing different amount of ionic liquids is shown in Figure 11. The conductivity increases with

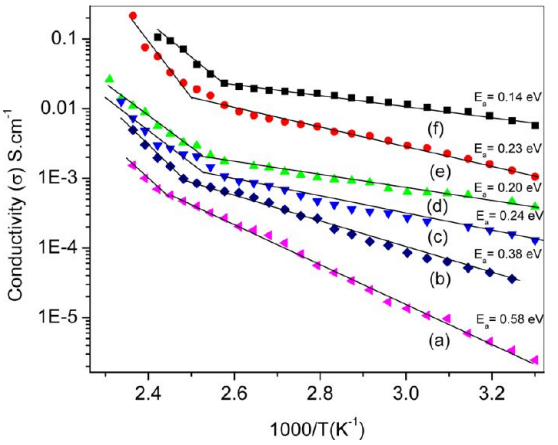

Figure 11. Temperature dependent conductivity of PVdF-HFP + x wt % IL gel membranes for (a) x = 30, (b) x = 40, (c) x = 50, (d) x = 60, (e) x = 70, and (e) x = 80, respectively.

temperature and follows an Arrhenius type thermally activated behavior in the lower temperature region. However, the σ vs $1/T$ plots shows significant changes in the conductivity values at a certain temperature which is essentially the melting temperature (T_m) of polymer where the amorphicity increases significantly. For most polymer electrolytes, it is known that the crystalline phase has lower conductivity than amorphous phase.[47] The PVdF-HFP is a semicrystalline polymer, and it is the melting of the crystalline phase at T_m which is responsible for the increase in conductivity at T_m. The value of melting temperature (T_m) changes with the amount of added IL as discussed earlier by us in the DSC results. The point of inflection (which is an indication of melting temperature T_m of polymers) obtained by conductivity plot is similar to the T_m obtained by the DSC plots of the PVdF-HFP + IL gels (see Figure 12, curves a and b).

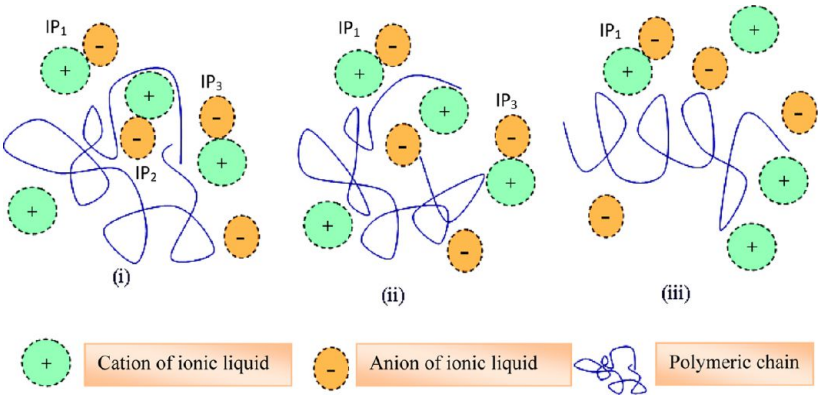

Figure 10. Schematic representation of the polymer chain breathing model for PVdF-HFP + IL gel membranes: (i) polymer gel membranes containing polymer chain, ion pairs (IP_1, IP_2, and IP_3, etc.), and free cations and anions derived from IL; (ii) opening up of folded polymer chain resulting in breaking up of one ion pair IP_2; (iii) further opening up of the polymer chain leading to breaking of more ion pairs such as IP_3. (see text for more detail).

dx.doi.org/10.1021/jp307694q | J. Phys. Chem. B 2013, 117, 897–906

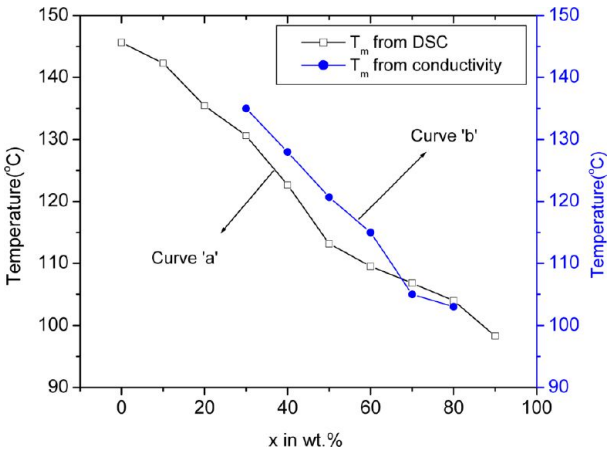

Figure 12. Melting temperature (T_m) of PVdF-HFP + x wt % IL gel membranes for different values of x obtained by DSC and point of inflection in the temperature dependent ionic conductivity plot.

The ionic conductivity at $T < T_m$ follows Arrhenius behavior and can be expressed as

$$\sigma = \sigma_o \exp(-E_a/kT) \quad (2)$$

where σ_o is the pre-exponential factor, E_a is the activation energy, k is the Boltzmann constant, and T is the temperature in K. The calculated values of activation energy (E_a) from log σ vs $1/T$ plots for PVdF-HFP + IL gel membranes are given in Figure 11. The activation energies are found to decrease with increasing amounts of IL in PVdF-HFP. This indicates easier ionic transport in PVdF-HFP + IL gel membranes having higher amounts of ionic liquid, as a result of increasing plasticization/amorphization of the polymeric membrane which was also indicated in the SEM/XRD results discussed earlier in this paper.

CONCLUSIONS

The gel polymer electrolyte membranes based on polymer PVdF-HFP and ionic liquid [BMIM][BF_4] have been prepared and studied. The amorphicity of the gel membranes was found to increase with increasing concentration of ionic liquid as confirmed by XRD/SEM/DSC studies due to its plasticization effect. FTIR and TGA studies show that the ionic liquid partly complexes with the polymer chain and partly remains as such in the membrane. The measured ionic conductivity of pure ionic liquid was interestingly found to increase on addition of low amounts of polymer (10 and 20 wt %) and then start decreasing monotonically with increasing polymer content due to viscosity enhancement. The variation of σ with the concentration of polymer PVdF-HFP in PVdF-HFP + IL gel membranes has been explained on the basis of the polymer chain breathing model. The opening up and folding of polymeric chain (as if breathing) lead to the breaking of ion pairs resulting in an increase in the number of mobile charge carriers (and hence σ). The temperature dependent ionic conductivity has also been studied and found to follow an Arrhenius type thermally activated behavior.

AUTHOR INFORMATION

Corresponding Author

* Tel. +91 542 2307308; fax +91 542 2368390; e-mail rksingh_17@rediffmail.com.

Notes

The authors declare no competing financial interest.

ACKNOWLEDGMENTS

One of the authors (S.C.) is thankful to the National Academy of Sciences, India for the award of position of Platinum Jubilee Senior Scientist, R.K.S is grateful to the U.G.C., New Delhi, India for providing the financial assistance to carry out this work. Shalu thanks the U.G.C., New Delhi, India for providing the project fellow fellowship, and S.K.C. is thankful to CSIR-New Delhi, India for the award of Senior Research Fellowship.

REFERENCES

(1) Croce, F.; Gerace, F.; Dautzemberg, G.; Passerini, S.; Appetecchi, G. B.; Scrosati, B. *Electrochim. Acta* **1994**, *39*, 2187−2194.
(2) Deepa, M.; Sharma, N.; Agnihotry, S. A.; Singh, S.; Lal, T.; Chandra, R. *Solid State Ionics* **2002**, *152*−*153*, 253−258.
(3) Michael, M. S.; Prabaharan, S. R. S. *J. Power Sources* **2004**, *136*, 408−415.
(4) Saito, Y.; Kataoka, H.; Capiglia, C.; Yamamoto, H. *J. Phys. Chem. B* **2000**, *104*, 2189−2192.
(5) Ferrari, S.; Quartarone, E.; Mustarelli, P.; Magistris, A.; Fagnoni, M.; Protti, S.; Gerbaldi, C.; Spinella, A. *J. Power Sources* **2010**, *195*, 559−556.
(6) Fernicola, A.; Weise, F. C.; Greenbaum, S. G.; Kagimoto, J.; Scrosati, B.; Soleto, A. *J. Electrochem. Soc.* **2009**, *156*, A514−A520.
(7) Liang, Y. H.; Wang, C. C.; Chen, C. Y. *Electrochim. Acta* **2006**, *52*, 527−537.
(8) Saikia, D.; Kumar, A. *Eur. Polym. J.* **2005**, *41*, 563−568.
(9) Pandey, G. P.; Agrawal, R. C.; Hashmi, S. A. *J. Power Sources* **2009**, *190*, 563−572.
(10) Asmara, S. N.; Kufian, M. Z.; Majid, S. R.; Arof, A. K. *Electrochim. Acta* **2011**, *57*, 91−97.
(11) Stallworth, P. E.; Greenbaun, S. G.; Croce, F.; Slane, S.; Salomon, M. *Electrochim. Acta* **1995**, *40*, 2137−2141.
(12) Dissanayake, M. A. K. L.; Bandari, L. R. A. K.; Bokalwala, R. S. P.; Jaythilaka, P. A. R. D.; Ileperumd, O. A.; Somasundaram, S. *Mater. Res. Bull.* **2002**, *37*, 867−864.
(13) Martinelli, A.; Matic, A.; Jacobsson, P.; Borjesson, L.; Fernicola, A.; Panero, S.; Scrosati, B.; Ohno, H. *J. Phys. Chem. B* **2007**, *111*, 12462−12467.
(14) Tsunemi, K.; Ohno, H.; Tsuchidd, E. *Electrochim. Acta* **1983**, *28*, 833−837.
(15) Egashira, M.; Todo, H.; Yoshimoto, N.; Morita, M. *J. Power Sources* **2008**, *178*, 729−735.
(16) Bansal, D.; Cassel, F.; Croce, F.; Hendrickson, H.; Plichta, E.; Salomon, M. J. *Phys. Chem. B* **2005**, *109*, 4492−4496.
(17) Matsumoto, K.; Sogabe, S.; Endo, T. *Polym. Chem.* **2012**, *50*, 1317−1324.
(18) Ohno, H. *Electrochemical Aspects of Ionic Liquids*; John Wiley & Sons, Inc.: Hoboken, NJ, 2005.
(19) An, Y.; Ching, X.; Zuo, P.; Liao, L.; Xin, G. *Mater. Chem. Phys.* **2011**, *128*, 250−255.
(20) Chaurasia, S. K.; Singh, R. K.; Chandra, S. *Solid State Ionics* **2011**, *183*, 32−39.
(21) Shin, J. H.; Henderson, W. A.; Passerini, S. *J. Electrochem. Soc.* **2005**, *152*, A978−A983.
(22) Kim, K. S.; Park, S. Y.; Choi, S.; Lee, H. *J. Power Sources* **2006**, *155*, 385−390.
(23) Schafer, T.; Di Paolo, R. E.; Franco, R.; Crespo, J. G. *Chem. Commun.* **2005**, 2594−2596.
(24) Hong, S. U.; Park, D.; Ko, Y.; Baek, I. *Chem. Commun.* **2009**, 7227−7229.
(25) Jonson, J. C.; Friess, K.; Clorizia, G.; Schauer, J.; Izak, P. *Macromolecules* **2011**, *44*, 39−45.
(26) Fuller, J.; Breda, A. C.; Carlin, R. T. *Electroanal. Chem.* **1998**, *459*, 29−34.

(27) Yeon, S. H.; Kim, K. S.; Choi, S.; Cha, J. H.; Lee, H. *J. Phys. Chem. B* **2005**, *109*, 1728−1735.
(28) Miao, R.; Liu, B.; Zhy, Z.; Liu, Y.; Li, J.; Wang, X.; Li, O. *J. Power Sources* **2008**, *184*, 420−426.
(29) Stephan, A. H.; Nahm, K. S.; Kulandainathan, M. A.; Ravi, G.; Wilson, J. *Eur. Polym. J.* **2006**, *42*, 1728−1734.
(30) Tian, X.; Jiang, X.; Zhu, B.; Xu, Y. *J. Membr. Sci.* **2006**, *279*, 479−486.
(31) Kobayashi, M.; Tashiro, K.; Tadokor, H. *Macramolecules* **1975**, *8*, 158−171.
(32) Li, Z.; Su, G.; Gao, D.; Wang, X.; Li, X. *Electrochim. Acta* **2004**, *49*, 4633−4639.
(33) Abberent, S.; Plestil, J.; Hlavata, D.; Lindgren, J.; Teganfeldt, J.; Wendsjo, A. *Polymer* **2001**, *42*, 1407−1416.
(34) Wang, K.; Lee, H.; Cooper, R.; Liang, H. *Appl. Phys. A: Mater. Sci. Process.* **2009**, *95*, 435−441.
(35) Simoes, R. D.; Job, A. E.; Chinaglia, D. L.; Zucolotto, V.; Camargo-Filho, J. C.; Alves, N.; Giacometti, J. A.; Oliveira, O. N., Jr.; Constantino, C. J. L. *J. Raman Spectrosc.* **2005**, *36*, 1118−1124.
(36) Heimer, N. E.; Sesto, R. E.D.; Heng, Z.; Wilkes, J. S.; Carper, W. R. *J. Mol. Liq.* **2006**, *124*, 84−95.
(37) Shi, J.; Wu, P.; Yan, F. *Langmuir* **2010**, *26*, 11427−11434.
(38) Jeon, Y.; Sung, J.; Seo, C.; Lim, H.; Cheong, H.; Kong, M.; Moon, B.; Ouchi, Y.; Kim, D. *J. Phys. Chem. B* **2008**, *112*, 4735−4740.
(39) Chaurasia, S. K.; Singh, R. K.; Chandra, S. *J. Polym. Sci., Part B: Polym. Phys.* **2011**, *49*, 291−300.
(40) Freitas, F. S.; Jilian, N. F.; Ito, I. B.; Paoli, M.; Nogueira, A. *Appl. Mater. Interfaces* **2009**, *1*, 2870−2877.
(41) Li, Z.; Jiang, J.; Lei, G.; Gao, D. *Polym. Adv. Technol.* **2006**, *17*, 604−607.
(42) Peakfit is a commercially available product from Seasolve Software Inc.
(43) Costa, C. M.; Rodrigues, L. C.; Sencadas, V.; Silva, M. M.; Rocha, J. G.; Lanceros-Mendez, S. *J. Membr. Sci.* **2012**, *407−408*, 193−201.
(44) Grillone, A. M.; Panero, S.; Retamal, B. A.; Scrosati, B. *J. Electrochem. Soc.* **1999**, *146*, 27−31.
(45) Patel, M.; Gnanavel, M.; Bhattacharyya, A. J. *J. Mater. Chem.* **2011**, *21*, 17419−17424.
(46) Chandra, S.; Sekhon, S. S.; Srivastava, R.; Arora, N. *Solid State Ionics* **2002**, *154−155*, 609−619.
(47) Grey, F. M. *Solid Polymer Electrolytes: Fundamental and Technological Applications*; VCH Publishers: New York, 1991.